Applied Catalysis B: Environmental 162 (2015) 217–226

Contents lists available at ScienceDirect

Applied Catalysis B: Environmental

journal homepage: www.elsevier.com/locate/apcatb

Microwave irradiated nickel nanoparticles on Vulcan XC-72R carbon black for methanol oxidation reaction in KOH solution

R.M. Abdel Hameed*, Rabab M. El-Sherif

Chemistry Department, Faculty of Science, Cairo University, Giza, Egypt

ARTICLE INFO

Article history:
Received 5 April 2014
Received in revised form 25 June 2014
Accepted 30 June 2014
Available online 8 July 2014

Keywords:
Methanol
Nickel-based electrocatalyst
Microwave irradiation
KOH
Fuel cells

ABSTRACT

Ni/C electrocatalysts were prepared by chemical deposition of nickel nanoparticles on Vulcan XC-72R carbon black using microwave irradiation technique. The time of microwave irradiation during the reduction step and nickel weight percentage were varied. This was found to affect the morphology of formed Ni/C powder as shown by TEM analysis. Increasing nickel weight percentage results in the formation of more aggregated deposits. The electrocatalytic activity of different Ni/C samples towards methanol oxidation reaction in KOH solution was studied by applying cyclic voltammetry, chronoamperometry and electrochemical impedance spectroscopic techniques. Ni/C electrocatalyst containing 30 wt.% Ni [Ni/C-30] shows 5.2 times higher electrocatalytic activity than that with 10 wt.% Ni [Ni/C-10]. Heating Ni/C powder into microwave oven using the pulse mode of 30 s on/10 s off forms the most stable electrocatalyst for prolonged oxidation reaction. Electrochemical impedance measurements show that Ni/C-30 electrocatalyst has the lowest impedance value of 0.022 kΩ cm^2, while the highest one is for Ni/C-10 [0.331 kΩ cm^2] in (0.4 M methanol + 0.5 M KOH) solution at 500 mV. It confirms that Ni/C-30 has the highest electrocatalytic activity towards methanol oxidation reaction.

1. Introduction

Electrocatalytic energy-conversion processes are aimed to participate in developing new sustainable technologies to overcome the global warming and the continuous need to fossil fuels [1–3]. Direct methanol fuel cells (DMFCs) have been widely studied as a promising future technology because they possess high energy density, low-to-zero pollutant emissions and availability of methanol fuel [4]. Pt is mostly used as an anode material in DMFCs; however, the slow kinetics of methanol oxidation reaction at its surface in acid medium represents a major problem [5–8]. This may be a result of continuous deactivation of its surface by poisoning intermediates, mainly CO molecules [9]. Moreover, the limited supply of Pt and its cost price impede its development in DMFCs [10]. Therefore, many efforts have been directed to investigate low cost non-noble metals as electrocatalysts for methanol oxidation reaction in alkaline medium [11,12]. Nickel-based materials showed high electrochemical performance with high stability in alkaline solution. They include nickel and nickel alloys [13–15], nickel hydroxide [16], nickel complexes [17] and nickel doped materials [18].

The preparation of nanoparticles has received significant attention in recent decades because of their unique physical and chemical properties [19,20]. Many methods have been reported for the synthesis of metallic nanoparticles including the impregnation [21], colloidal deposition [22], supercritical fluid [23] and electrodeposition [24]. The impregnation and colloidal methods are usually adopted. The impregnation method is simple and straightforward; however, it is somewhat difficult to control the nanoparticles size to get small particles with narrow size distribution. On the other hand, good dispersion of ultrafine Pt nanoparticles with sharp size distribution could be produced using the colloidal method. Unfortunately, it is complex and time-consuming process which limits its application and affects the total mass of the produced catalyst.

Microwave irradiation was widely used for nanomaterials preparation. A glass or plastic reaction container was applied to uniformly heat the substance, leading to a more homogeneous nucleation and shorter crystallization time with respect to the conventional heating methods. Pt–NiO/C electrocatalyst, prepared using the microwave irradiation during the reduction step of Pt ions, showed three folds increment in methanol oxidation peak current density with a potential shift in the positive direction by 53 mV, relative to that at the same electrocatalyst, prepared using the impregnation method [25]. Slower current density decay was

* Corresponding author. Tel.: +20 1145565646; fax: +235727556.
E-mail addresses: randa311eg@yahoo.com, noura31176@hotmail.com (R.M. Abdel Hameed).

http://dx.doi.org/10.1016/j.apcatb.2014.06.057
0926-3373/

observed in the chronoamperogram of Pt–CuO/C electrocatalyst, prepared by the microwave method, reflecting a lower degree of surface poisoning [26]. Sakthivel et al. [27] have studied the effect of various preparation parameters of microwave-assisted polyol reduction method of Pt/MWCNTs electrocatalyst on Pt particle size, uniformity of nanoparticles distribution and overall Pt loading. They include the surfactant to Pt precursor ratio, the heating time and temperature of microwave irradiation. This in turn affected the performance of Pt/MWCNTs in single DMFC measurements. The power density of surfactant stabilized cathode catalyst was two times higher than for an unstabilized catalyst. Song et al. [28] have also found that the operation mode of microwave heating affects the reduction efficiency. The pulse mode is preferred over the continuous one. Pt/C catalyst, prepared using the pulse microwave mode of 10 s on/10 s off for 5 pulses, showed the best electrocatalytic activity towards methanol and ethanol electrooxidation.

Here in our study, Ni/C electrocatalyst is chemically reduced using sodium borohydride as the reducing agent with the aid of microwave heating irradiation. The heating time during the pulse mode and the weight percentage of nickel are varied during the preparation step. The catalyst morphology and its particle size are determined using transmission electron microscopy. Energy dispersive X-ray analysis, on the other hand, confirms its chemical composition. The electrocatalytic performance of different Ni/C electrocatalysts is examined towards methanol oxidation reaction in KOH solution. Various electrochemical techniques are employed including cyclic voltammetry, chronoamperometry and impedance spectroscopy.

2. Experimental

2.1. Chemicals

Vulcan XC-72R carbon black was purchased from Cabot Corp., USA with a specific surface area (BET) of 240 $m^2\ g^{-1}$ and an average particle size of 40 nm. Nafion (perfluorosulphonic acid-PTFE copolymer, 5 wt.% solution) was obtained from Sigma–Aldrich, Germany. All other chemical reagents [methanol, KOH, $NaBH_4$ and $NiCl_2.6H_2O$] in this work were of analytical grade and used as received without further purification. Double distilled water was used for electrodes washing and preparation of all aqueous solutions.

2.2. Preparation of different Ni/C electrocatalysts

A suspended solution of Vulcan XC-72R carbon black was sonicated for 30 min. Nickel chloride solution was then added with stirring for another 30 min. The nickel metal loading was kept as 30 wt.%. Sodium borohydride solution with a molar ratio of 70 times higher than that of nickel metal was added dropwisely to the above mixture with constant stirring within 30 min. Microwave irradiation was applied to help accelerating the reduction process via a household microwave oven (Caira CA-MW 1025, touch pad digital control, 50 MHz, 1400 W). Ni/C electrocatalysts were prepared using the pulse mode of microwave heating. It was divided into separate pulses with each one followed by a pause for 10 s. The total working time was kept constant as 5 min. The pulse time was varied as 10, 20, 30 and 50 s in Ni/C-a, Ni/C-b, Ni/C-c and Ni/C-d electrocatalysts, respectively. Ni/C powder was then filtered and washed with double distilled water for 6 times. It was then dried in an air oven at 80 °C for 6 h. In addition, the nickel weight percentage was altered in another set of Ni/C electrocatalysts as 10, 20, 40 and 60 using the pulse mode of (20 s on/10 s off). The corresponding electrocatalysts were designated as Ni/C-10, Ni/C-20, Ni/C-40 and Ni/C-60, respectively.

2.3. Physical characterization of Ni/C electrocatalysts

The electrocatalyst morphology and its particle size could be determined using transmission electron microscopy (TEM). JEOL-JEM 2010 transmission electron microscope was working at an accelerating voltage of 160 kV. The measured sample was suspended in double distilled water and sonicated for 480 s in ultra 8050-H Clifton. A drop of this suspension was then dispersed over copper grid coated with carbon film and left to dry in air. Gatan program was used to estimate nickel nanoparticles size. Energy dispersive X-ray spectroscopy (EDX) was applied to determine the chemical composition of Ni/C electrocatalyst. EDX analysis unit "INCA X-sight, OXFORD instruments, England" was used. It was attached to scanning electron microscope "JXA-840A, Electron Prob Microanalyzer, JEOL, Japan".

2.4. Electrode fabrication and electrochemical measurements

Commercial carbon rod with a surface area of 0.5 cm^2 was used to support Ni/C powder. It was first polished with emery papers in different grades and washed with double distilled water and acetone. This carbon electrode would be activated by cyclization in 0.5 M H_2SO_4 solution in the potential window from −800 to +1600 mV versus Hg/Hg_2SO_4/1.0 M H_2SO_4 (MMS) for 50 cycles at a scan rate of 50 mV s^{-1}. The catalyst ink was prepared by dispersing 10 mg Ni/C powder in 5 ml isopropyl alcohol with sonication for 5 min. The commercial carbon rod was then coated with 0.5 ml of this suspension. The electrocatalyst powder was then fixed on the carbon surface by adding 0.1 ml Nafion solution. It was left to dry in air and stored overnight in a desiccator before use.

The electrochemical measurements were performed using Voltamaster 6 potentiostat. A conventional three-electrodes system was employed. It consists of the commercial carbon rod coated with nickel nanoparticles/Vulcan XC-72R carbon black powder as the working electrode. Pt wire and Hg/HgO/1.0 M NaOH (MMO) were used as the auxiliary and reference electrodes, respectively. All potentials in this work are referred to (MMO) [its potential is equivalent to +140 mV (NHE)]. Cyclic voltammograms and chronoamperograms were recorded in 0.5 M KOH solution as a supporting electrolyte solution with adding different methanol concentrations. The studied potential range in cyclic voltammetric measurements was chosen from −200 to 1100 mV at a scan rate of 10 mV s^{-1}. The electrochemical impedance spectroscopic study has been carried out using the IM6d.AMOS system (Zahner Elektrik GmbH & Co., Kronach, Germany). It was operated at constant dc potential value of 500 mV with ac voltage amplitude of 10 mV. The frequency range of 0.1–1 × 10^4 Hz was employed. Before each experiment, the working electrode was immersed in the test solution for 300 s at 500 mV. The data were theoretically fitted according to the proposed equivalent circuit models using a complex non-linear least squares (CNLS) circuit fitting software. All electrochemical measurements were operated in aerated electrolytes at room temperature of 30 °C ± 0.2.

3. Results and discussion

The weight percentage of nickel in Ni/C electrocatalyst was found to affect its surface morphology as observed in Fig. 1. Carbon black appears as spherical particles with a mean diameter of 35 nm. Ni nanoparticles were uniformly distributed on carbon surface with a mean diameter of 6 nm in Ni/C samples containing lower metal loadings [Ni/C-10 in Fig. 1a]. Increasing the nickel weight percentage results in the formation of more dense deposits [Ni/C-30 in Fig. 1b, Ni/C-40 in Fig. 1c and Ni/C-60 in Fig. 1d]. Energy dispersive

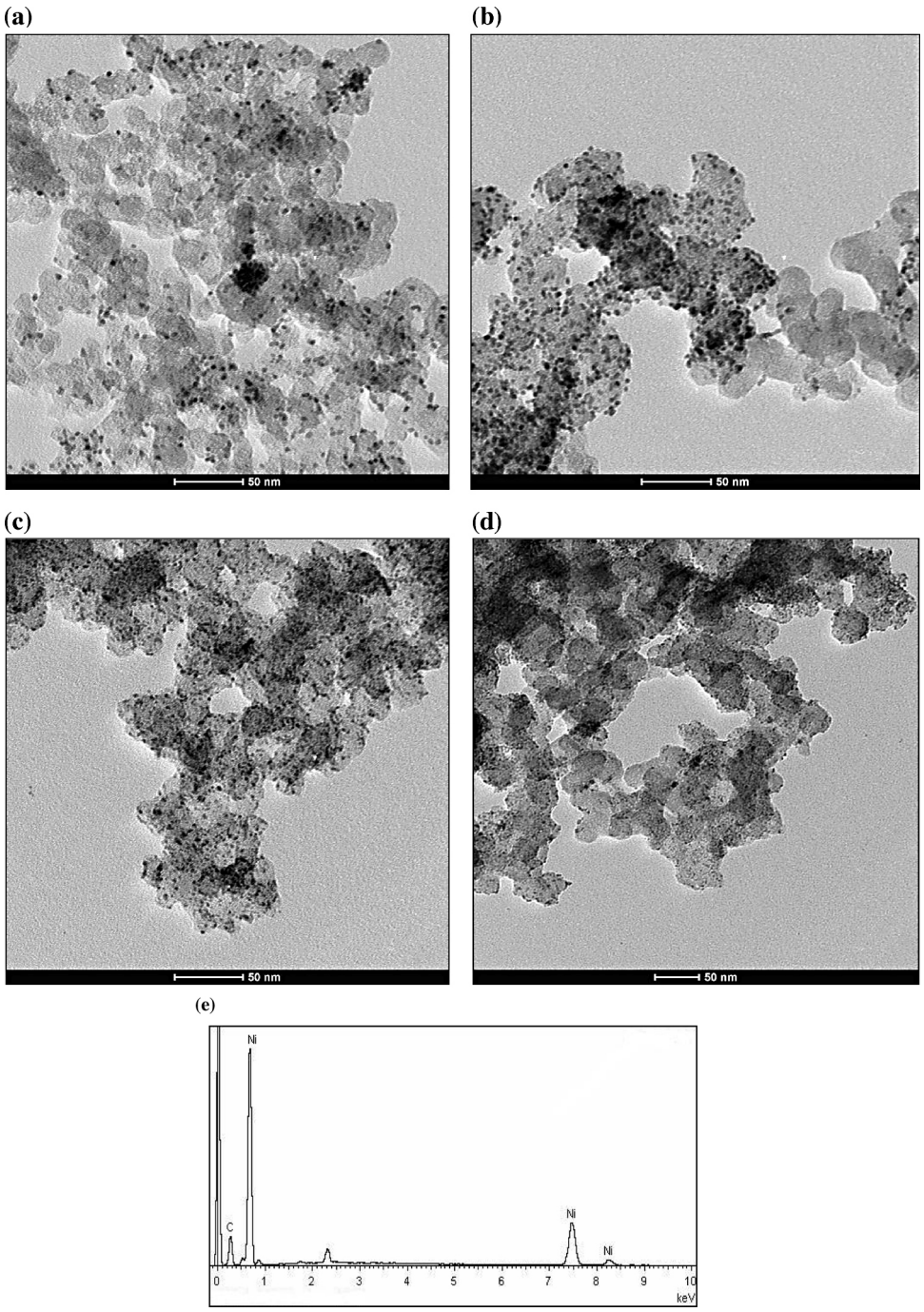

Fig. 1. TEM images of (a) Ni/C-10, (b) Ni/C-30, (c) Ni/C-40 and (d) Ni/C-60 electrocatalysts. (e) Energy dispersive X-ray spectrum of Ni/C-30 electrocatalyst.

X-ray spectrum of Ni/C-30 electrocatalyst in Fig. 1e confirms the deposition of nickel metal on carbon Vulcan XC-72R powder.

Fig. 2 shows the cyclic voltammogram of Ni/C-30 electrocatalyst in 0.5 M KOH solution at 10 mV s^{-1}. An increase in the current density is observed starting at a potential value of 473 mV to get an oxidation peak at a potential value of 609 mV. It corresponds to $Ni(OH)_2$ species transformation to NiOOH based on the following equation [21,22,29,30]:

$$Ni(OH)_2 + OH^- \leftrightarrow NiOOH + H_2O + e^- \quad (1)$$

Oxygen starts to evolve at a potential value of 692 mV with a high current density value. The formed NiOOH is reduced in the backward direction at a potential value of 239 mV.

The cyclic voltammograms of Ni/C-30 electrocatalyst in 0.5 M KOH solution at different scan rates are represented in Fig. 3A and A′. The current density of $Ni(OH)_2$/NiOOH redox couple increases with increasing the scan rate. In addition, the potential value of the anodic oxidation peak is shifted in the positive direction, while the cathodic reduction peak shows more negative potential values as the scan rate increases. The electron transfer coefficient (α) and electron transfer rate constant (k_s) can be estimated using Laviron's theory that manifests the slow electron transfer of attached electroactive species [31] according to the following equations:

$$E_{pa} = E_o + RT/\left\{(1-\alpha)nF\right\} \times \ln\left\{(1-\alpha)nF\upsilon/RTk_s\right\} \quad (2)$$

$$E_{pc} = E_o + RT(\alpha nF) \times \ln\left(\alpha nF\upsilon/RTk_s\right) \quad (3)$$

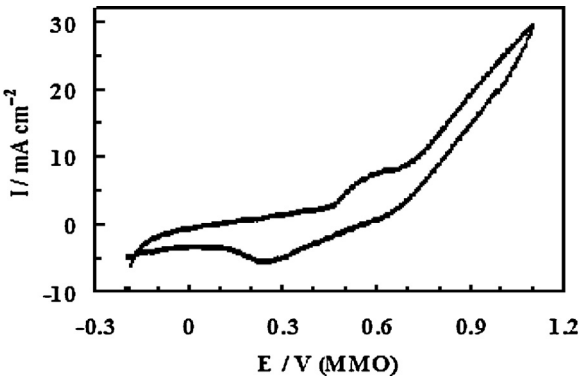

Fig. 2. Cyclic voltammogram of Ni/C-30 electrocatalyst in 0.5 M KOH solution at 10 mV s^{-1}.

$$\ln k_s = \alpha \ln(1-\alpha) + (1-\alpha)\ln\alpha - \ln\left(\frac{RT}{nF\upsilon}\right) - \frac{\alpha(1-\alpha)nF\Delta E}{RT} \quad (4)$$

where E_{pa} and E_{pc} are the anodic and cathodic peak potential values in V, respectively, E_o is the standard electrode potential, R is the universal gas constant (8.314 J mol^{-1} K^{-1}), T is the absolute temperature in K, F is Faraday's constant (96485.3 C mol^{-1}), n is the electron transfer number, υ is the scan rate in V s^{-1} and k_s is the electron transfer rate constant in s^{-1}. The anodic and cathodic peak potential values are drawn as a function of the natural logarithm of the scan rate at Ni/C-30 electrocatalyst in Fig. 3B. A linear plot is observed at higher scan rates [200–900 mV s^{-1}]. The slope of this line is substituted into Eqs. (2) and (3) to calculate the electron transfer coefficient value (α) at Ni/C-30 electrocatalyst as 0.509. Based on this α value and using Eq. (4), the electron transfer rate constant (k_s) at Ni/C-30 electrocatalyst is 7.54×10^{-2} s^{-1}.

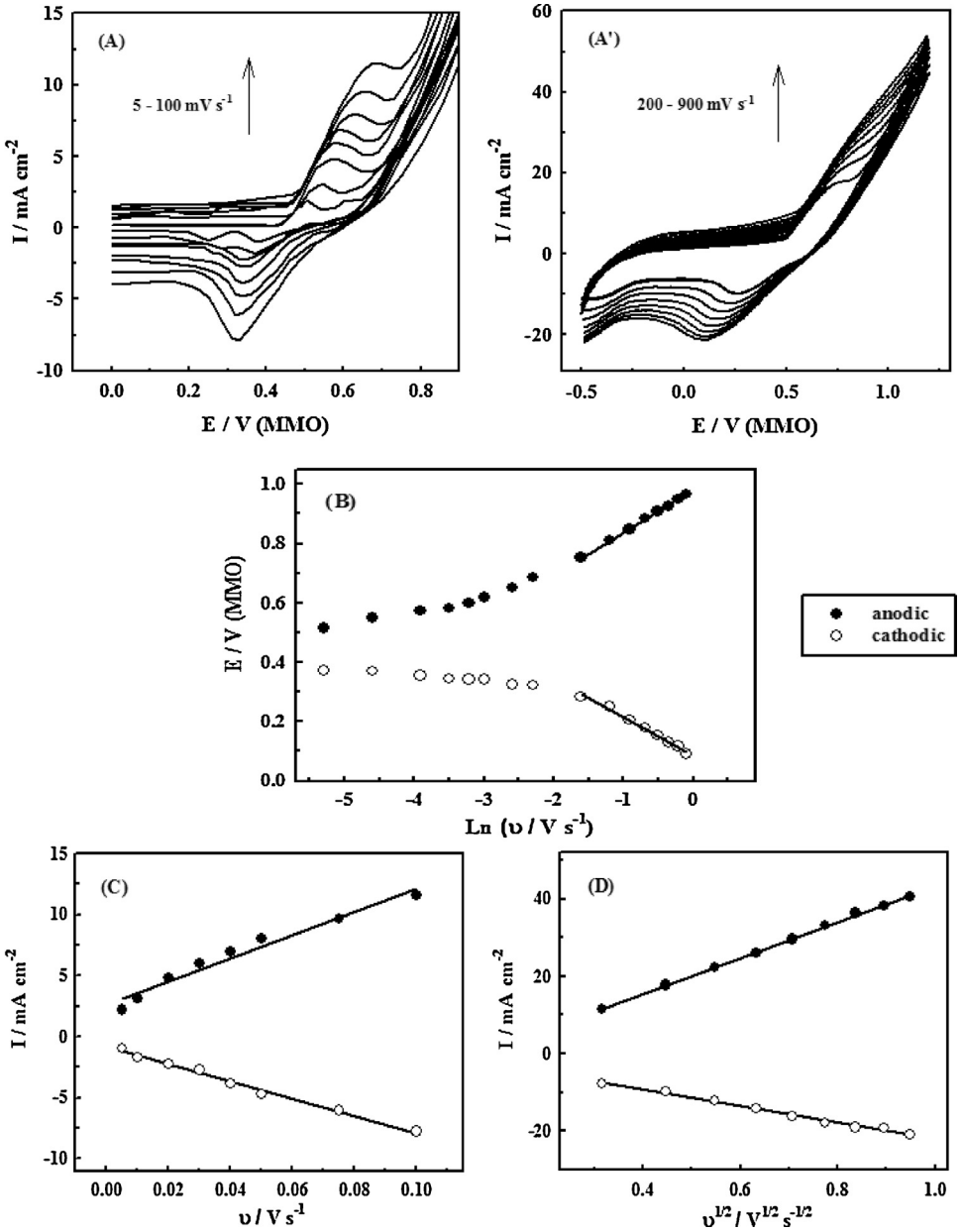

Fig. 3. (A, A′) Cyclic voltammograms of Ni/C-30 electrocatalyst in 0.5 M KOH solution at scan rates of 5, 10, 20, 30, 40, 50, 75, 100, 200, 300, 400, 500, 600, 700, 800 and 900 mV s^{-1}. (B) The dependence of the anodic and cathodic peak potential values on the natural logarithm of the scan rate. The linear dependence of the anodic and cathodic peak current density on the scan rate at lower values (5–100 mV s^{-1}) (C) and on the square root of the scan rate at higher values (100–900 mV s^{-1}) (D).

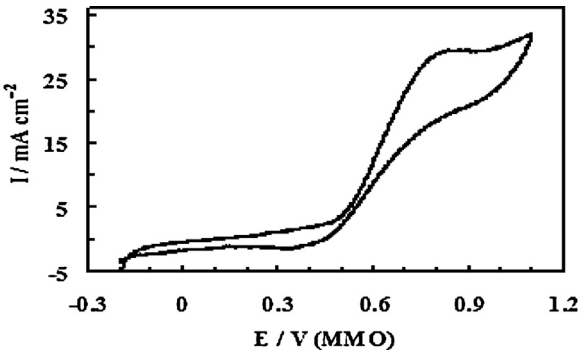

Fig. 4. Cyclic voltammogram of Ni/C-30 electrocatalyst in (0.4 M methanol + 0.5 M KOH) solution at 10 mV s^{-1}.

Fig. 3C displays the variation of the current density values of the anodic and cathodic peaks of $Ni(OH)_2$/NiOOH redox couple at Ni/C-30 electrocatalyst with the scan rate at lower values from 5 to 100 mV s^{-1}. A linear relationship is obtained as a result of the electrochemical activity of immobilized redox species at the surface of modified electrodes. From the slope of this relation and using the following equation, the electrode surface coverage (Γ^*) can be estimated [32]:

$$I_p = \left(\frac{n^2F^2}{4RT}\right)\upsilon A\Gamma^* \quad (5)$$

where I_p is the peak current in Ampere, A is the electrode surface area in cm^2 and Γ^* is the surface coverage of redox species in mol cm^{-2}. The average of the anodic and cathodic sides is taken to get Γ^* value of 8.90×10^{-8} mol cm^{-2}. When the scan rate values are higher than 100 mV s^{-1}, the current density values of $Ni(OH)_2$/NiOOH redox couple are proportional to the square root of the scan rate. This relation in Fig. 3D indicates that a diffusion-controlled process prevails during the redox transition at the modified electrode.

The addition of 0.4 M methanol to 0.5 M KOH solution results in some changes in the cyclic voltammetric curve as noticed in Fig. 4. An increase in the current density is coincided with the start of NiOOH formation. Methanol oxidation peak is shown at a potential value of 860 mV with a current density of 30 mA cm^{-2}. The reduction peak of NiOOH after adding methanol shows very low current density with a potential shift in the positive direction. The above observations indicate that NiOOH species acts as a catalyst for methanol oxidation reaction.

The effect of varying the heating time of Ni/C electrocatalyst in microwave oven on its electrocatalytic activity towards methanol oxidation reaction was studied. The corresponding cyclic voltammograms in (0.4 M methanol + 0.5 M KOH) solution at 10 mV s^{-1} are displayed in Fig. 5. It is noticed that increasing the heating time of the pulse mode during nickel ions reduction results in an enhanced oxidation current density of Ni/C electrocatalyst. Ni/C-b electrocatalyst that was formed using a pulse mode of 20 s on/10 s off is more active than Ni/C-a [with a pulse mode of 10 s on/10 s off] by two-folds with a negative shift of its oxidation peak potential by 54 mV. When the heating time of Ni/C electrocatalyst is further prolonged, the oxidation reaction rate is lowered. It is apparent from the decreased current density and more positive potential values of its methanol oxidation peak. This result could be explained based on the increased efficiency of the metal reduction process with increasing the heating time in microwave oven. However, much prolonged heating time increases the agglomeration degree of nickel nanoparticles during their deposition on carbon surface [33].

The cyclic voltammograms of Ni/C electrocatalysts, containing different nickel weight percentages, in (0.4 M methanol + 0.5 M KOH) solution at 10 mV s^{-1} are displayed in Fig. 6. The methanol oxidation current density increases with increasing the weight percentage of nickel in Ni/C electrocatalyst. Ni/C-30 has the highest electrocatalytic activity with 5.2 times improved oxidation current density when compared to that at Ni/C-10 electrocatalyst. Further increase of the nickel amount in Ni/C electrocatalyst decays its catalytic performance. The increased agglomeration of nickel nanoparticles in our prepared Ni/C electrocatalysts with increasing their nickel content [as evidenced from TEM images in Fig. 1] tends to lower the corresponding electrocatalytic activity. Wang et al. [34] have concluded that as nickel amount in Ni–Al layered double hydroxide film modified electrode increases, the electroactive Ni(II) deposited on the electrode increases, leading to higher electrocatalytic activity. After the Ni:Al ratio reached 3:1, the oxidation current density of nickel modified electrode increases very slowly. Abdel Rahim et al. [35] have prepared nickel modified graphite electrode by potentiostatic deposition method for different time intervals. Low catalyst quantity showed high catalytic activity towards methanol oxidation reaction in KOH solution. However, the relatively thick nickel oxide films that were formed during nickel deposition for longer time can act as a barrier for methanol oxidation reaction.

Fig. 7a represents the chronoamperograms of methanol oxidation reaction at Ni/C-30 electrocatalyst in 0.5 M KOH solution containing various methanol concentrations ranging from 0.10 to 0.50 M. They are carried out at a potential step value of 700 mV for 1800 s. The oxidation current density rapidly decreases at the first 200 s in all chronoamperograms, followed by a steady state. As methanol concentration increases, the current density generally increases. The maximum value is obtained when 0.4 M methanol is added to the supporting electrolyte. Higher methanol concentration values result in a decreased catalytic activity. The steady state oxidation current density of Ni/C-30 electrocatalyst is plotted as a function of methanol concentration in Fig. 7b. Based on this observation, 0.4 M methanol was chosen as the optimum concentration to carry out further experiments.

The chronoamperograms of methanol oxidation reaction at Ni/C-30 electrocatalyst in 0.4 M methanol in KOH solution with different concentrations are represented in Fig. 8a at a potential step value of 700 mV for 1800 s. As KOH concentration increases, the steady state current density of methanol oxidation reaction would increase. A plot of this current density value as a function of KOH concentration in Fig. 8b is linear relationship. This confirms the dependence of the oxidation reaction mechanism on OH^- ions concentration. The order of methanol oxidation reaction with respect to KOH concentration can be calculated according to the following equation:

$$\text{Rate} \equiv \text{I} = kC^n \quad (6a)$$

$$\text{Log}\, I = \text{Log}\, k + n\,\text{Log}\, C \quad (6b)$$

where I is the steady state oxidation current density, k is the reaction rate constant, C is the concentration and n is the reaction order. Fig. 8c is the logarithmic relation between the oxidation current density of Ni/C-30 electrocatalyst and KOH concentration. Straight line is obtained with a slope value of 1.15. Therefore, methanol oxidation reaction at Ni/C-30 electrocatalyst is first order with respect to KOH concentration.

The stability of different Ni/C electrocatalysts during methanol oxidation reaction was examined using chronoamperometry in (0.4 M methanol + 0.5 M KOH) solution at a potential step value

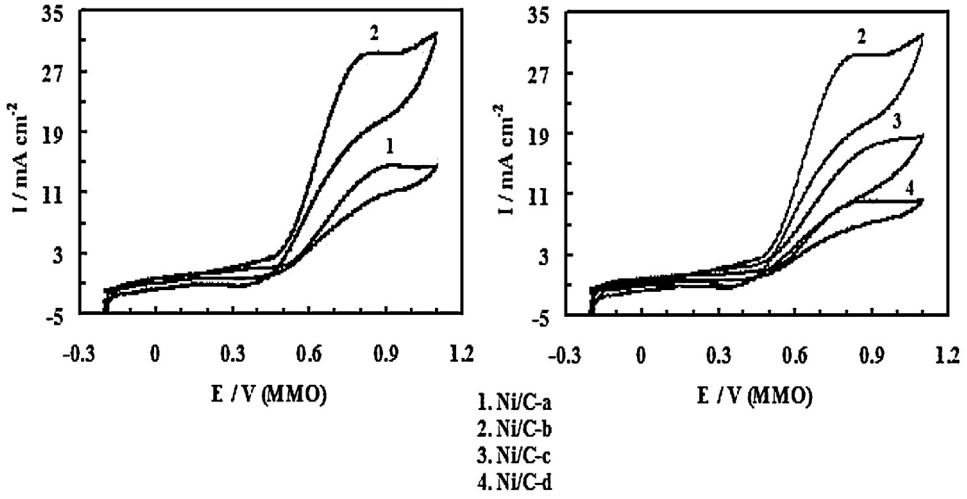

Fig. 5. Cyclic voltammograms of methanol oxidation reaction at Ni/C electrocatalysts, heated in microwave oven for different times, in (0.4 M methanol + 0.5 M KOH) solution at 10 mV s^{-1}.

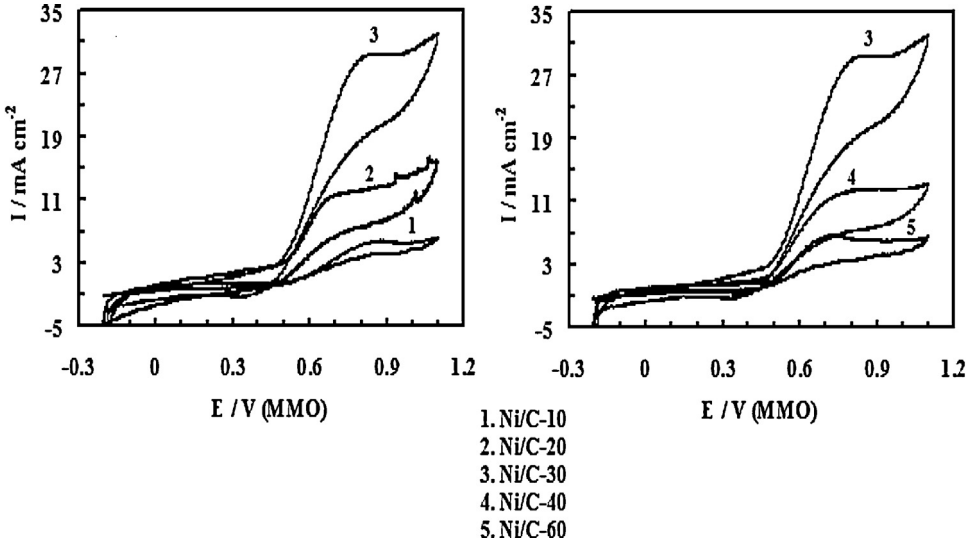

Fig. 6. Cyclic voltammograms of methanol oxidation reaction at Ni/C electrocatalysts, containing different nickel weight percentages, in (0.4 M methanol + 0.5 M KOH) solution at 10 mV s^{-1}.

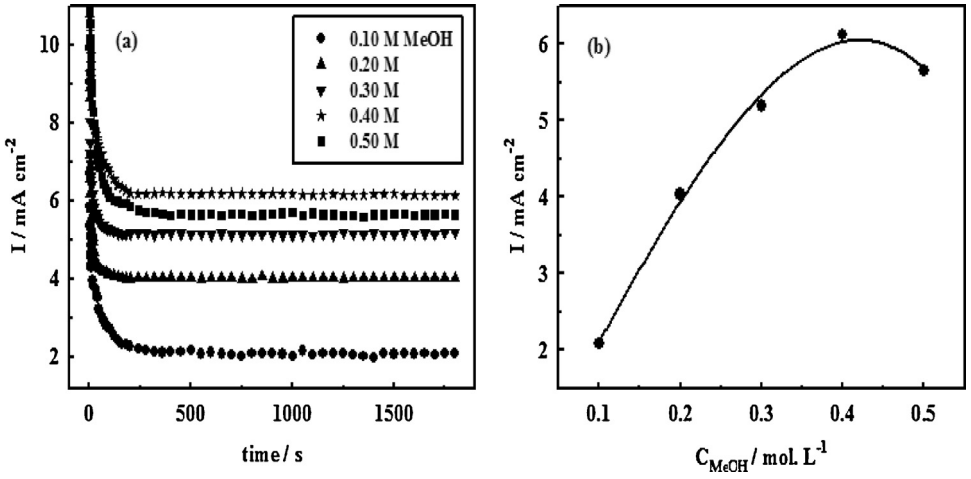

Fig. 7. (a) Chronoamperograms of methanol oxidation reaction at Ni/C-30 electrocatalyst in 0.5 M KOH solution containing different methanol concentrations at a potential step value of 700 mV for 1800 s. (b) Variation of the steady state oxidation current density of Ni/C-30 electrocatalyst as derived from section (a) after 1800 s as a function of methanol concentration.

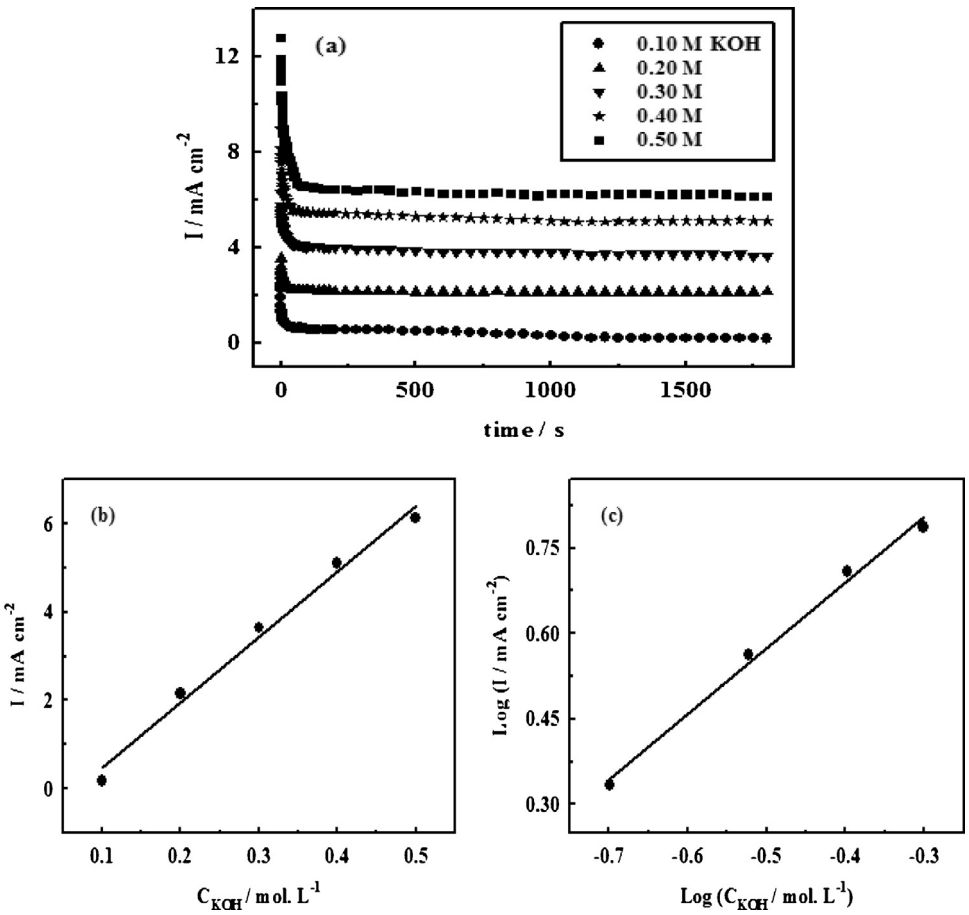

Fig. 8. (a) Chronoamperograms of methanol oxidation reaction at Ni/C-30 electrocatalyst in 0.4 M methanol in KOH solution with different concentrations at a potential step value of 700 mV for 1800 s. (b) Variation of the steady state oxidation current density of Ni/C-30 electrocatalyst as derived from section (a) after 1800 s as a function of KOH concentration. (c) The logarithmic relation for the data in section (b).

of 700 mV for 1800 s. Fig. 9a records these chronoamperograms for Ni/C electrocatalysts, heated for different time intervals in microwave oven. Increasing the heating time of Ni/C tends to enhance its stability. Ni/C-c electrocatalyst, heated in 30 s on/10 s off pulse mode shows the highest steady state oxidation current density. Longer heating times, however, retards the methanol oxidation reaction at Ni/C-d electrocatalyst. The variation of the steady state oxidation current density of Ni/C electrocatalysts, heated for different time intervals in microwave oven is clarified in Fig. 9b. The corresponding chronoamperograms for Ni/C electrocatalysts, containing different nickel weight percentages, are represented in Fig. 10a. Increasing the steady state oxidation current density is relevant to the increased nickel weight percentage. When Ni/C electrocatalyst contains 40 wt.% Ni, its maximum oxidation current density is attained. Lower catalytic activity is observed when the nickel loading in Ni/C electrocatalyst exceeds this value. Fig. 10b is the relation between the steady state oxidation current density and nickel weight percentage.

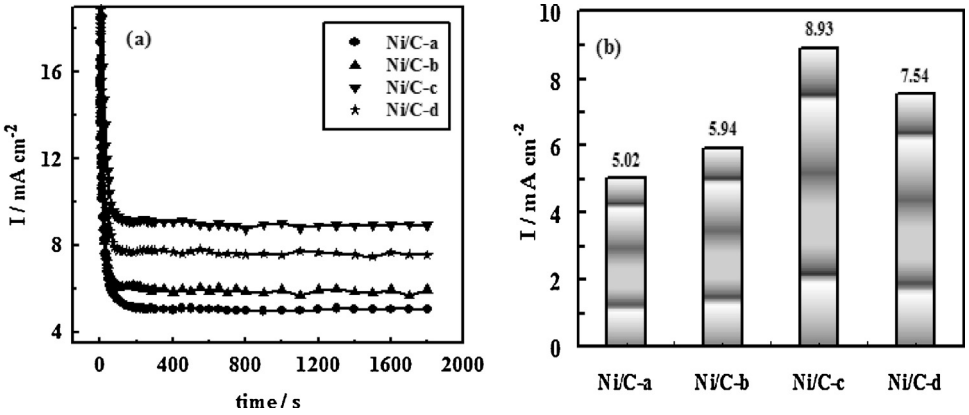

Fig. 9. (a) Chronoamperograms of methanol oxidation reaction at Ni/C electrocatalysts, heated for different microwave irradiation times, in (0.4 M methanol + 0.5 M KOH) solution at a potential step value of 700 mV for 1800 s. (b) Variation of the steady state oxidation current density of different Ni/C electrocatalysts as derived from section (a) after 1800 s as a function of microwave irradiation time.

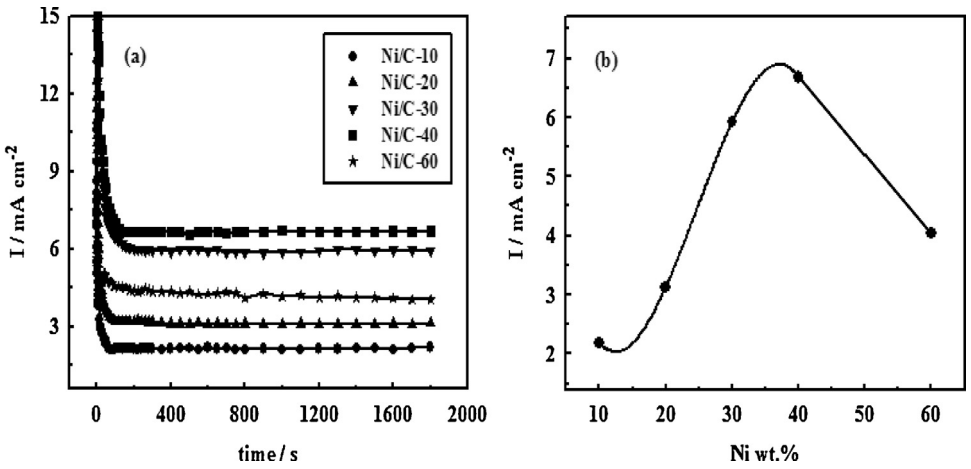

Fig. 10. (a) Chronoamperograms of methanol oxidation reaction at Ni/C electrocatalysts, containing different nickel weight percentages, in (0.4 M methanol + 0.5 M KOH) solution at a potential step value of 700 mV for 1800 s. (b) Variation of the steady state oxidation current density of different Ni/C electrocatalysts as derived from section (a) after 1800 s as a function of nickel weight percentage.

The catalytic activity of the prepared electrocatalysts for methanol oxidation reaction was also studied using EIS measurements. Fig. 11a and b represents the Nyquist and Bode diagrams, respectively of Ni/C-30 electrocatalyst in 0.5 M KOH solution in absence and in presence of 0.4 M methanol. A highly increased diameter of the electrocatalyst semicircle is observed in 0.5 M KOH solution in absence of methanol. This is supported by the corresponding electrochemical impedance parameters in Table 1. Fig. 12a shows the Nyquist diagrams of Ni/C electrocatalysts containing different nickel weight percentages in (0.4 M methanol + 0.5 M KOH) solution. They are consisted of two slightly depressed capacitive semicircles at high and low frequency values. The depressed semicircle in the high frequency region can be related to the combination of the charge transfer resistance and double layer capacitance. On the other hand, the adsorption of the reaction intermediates on the electrode surface may account for the low frequency semicircle. The relevant Bode plots for these nickel-based electrocatalysts are shown in Fig. 12b. The observed broad peak is related to the two depressed semicircles in the Nyquist plot. The equivalent circuit that fits this Nyquist diagram is depicted in Fig. 13. To obtain a satisfactory impedance simulation of methanol oxidation reaction, it is necessary to replace the capacitor C in the equivalent circuit with a constant phase element (CPE). The most widely accepted explanation for the presence of CPE behaviour and depressed semicircles on solid electrodes is microscopic roughness, causing an inhomogeneous distribution in the solution resistance as well as in the double layer capacitance [36]. In this electrical equivalent circuit, R_s, CPE and R_{ct} represent solution resistance, a constant phase element corresponding to the double layer capacitance and the charge transfer resistance, respectively. CPE_{ads} and R_{ads} are the electrical elements related to the adsorption of reaction intermediates. Total polarization resistance was shown as $R_p = R_{ct} + R_{ads}$. In this circuit, the charge transfer resistance of the electrode reaction is the parameter that describes how fast the rate of the charge transfer during methanol oxidation reaction is altered with varying nickel weight percentage, keeping the surface coverage of the intermediate constant. To corroborate the equivalent circuit, the experimental data are fitted to the equivalent circuit and the circuit elements are obtained. They are listed in Table 2 for the impedance spectra of methanol oxidation reaction at various Ni/C electrocatalysts containing different nickel weight percentages. As can be seen from Fig. 12a and the resistance values in Table 2, Ni/C-30 electrocatalyst shows the lowest diameter of the semicircles, while the highest one is for Ni/C-10. It emphasizes that Ni/C-30 has the highest electrocatalytic activity towards methanol oxidation reaction. Further increase of the nickel amount in Ni/C electrocatalyst decays its catalytic performance as evidenced from the increased charge transfer resistance values in Table 2. Methanol oxidation reaction is preceded by the surface adsorption step. Therefore, minimum adsorption resistance values strongly facilitate the kinetics of the Faradic electrooxidation process.

Fig. 14a shows the Nyquist diagrams of Ni/C electrocatalysts, heated in microwave oven for different times, in (0.4 M methanol + 0.5 M KOH) solution. It is noticed that increasing the heating time of the pulse mode during nickel ions reduction results in an enhanced performance of Ni/C electrocatalyst. The lowest diameter of the semicircles is recorded for Ni/C-b, whereas

Table 1
Electrochemical impedance parameters of Ni/C-30 electrocatalyst in 0.5 M KOH solution in absence and in presence of 0.4 M methanol.

Solution	R_s (Ω)	CPE (μF cm^{-2})	n_1	R_{ct} (kΩ cm^2)	C_{ads} (μF cm^{-2})	n_2	R_{ads} (kΩ cm^2)
0.5 M KOH	11.9	3.4	0.67	0.025	126.6	0.82	0.334
(0.4 M methanol + 0.5 M KOH)	7.3	3.4	0.68	0.005	200.4	0.73	0.022

Table 2
Electrochemical impedance parameters of Ni/C electrocatalysts, containing different nickel weight percentages, in (0.4 M methanol + 0.5 M KOH) solution.

Electrocatalyst	R_s (Ω)	CPE (μF cm^{-2})	n_1	R_{ct} (kΩ cm^2)	C_{ads} (μF cm^{-2})	n_2	R_{ads} (kΩ cm^2)
Ni/C-10	10.6	2.35	0.68	0.009	156.0	0.78	0.331
Ni/C-20	5.2	1.64	0.70	0.007	188.3	0.80	0.103
Ni/C-30	7.3	3.40	0.68	0.005	200.4	0.73	0.022
Ni/C-40	9.9	2.18	0.69	0.006	182.6	0.75	0.189
Ni/C-60	10.3	3.00	0.99	0.007	174.2	0.76	0.294

Table 3
Electrochemical impedance parameters of Ni/C electrocatalysts, heated in microwave oven for different times, in (0.4 M methanol + 0.5 M KOH) solution.

Electrocatalyst	R_s (Ω)	CPE (μF cm^{-2})	n_1	R_{ct} (kΩ cm^2)	C_{ads} (μF cm^{-2})	n_2	R_{ads} (kΩ cm^2)	W (kΩ s$^{-1/2}$)
Ni/C-a	17.1	4.5	0.64	0.006	215.0	0.79	0.160	–
Ni/C-b	7.3	3.4	0.68	0.005	200.4	0.73	0.022	–
Ni/C-c	9.9	5.2	0.72	0.004	211.0	0.89	0.156	48.34
Ni/C-d	16.3	5.8	0.68	0.004	185.6	0.87	0.178	1.78

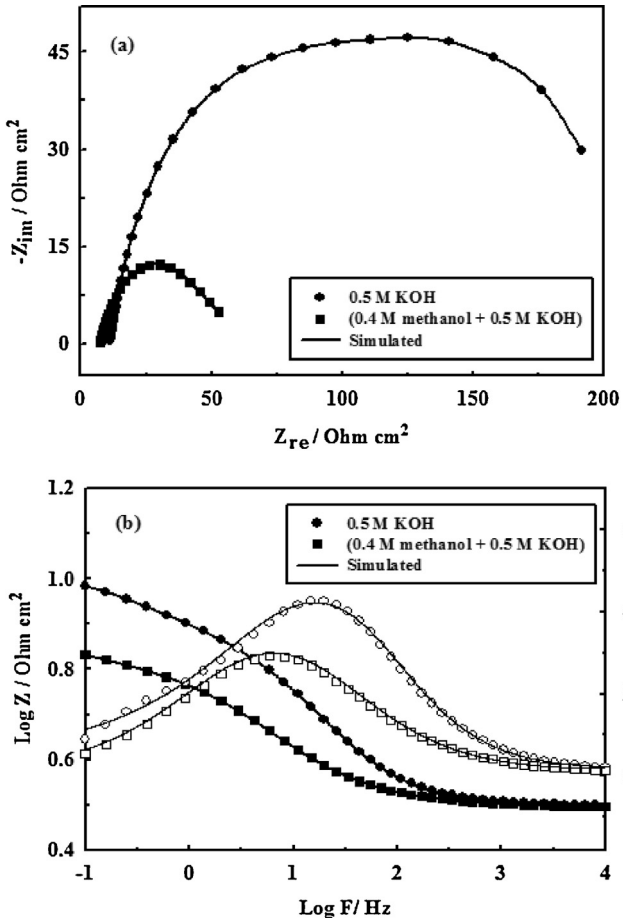

Fig. 11. (a) Nyquist and (b) Bode plots of Ni/C-30 electrocatalyst in 0.5 M KOH solution in absence and in presence of 0.4 M methanol at 500 mV.

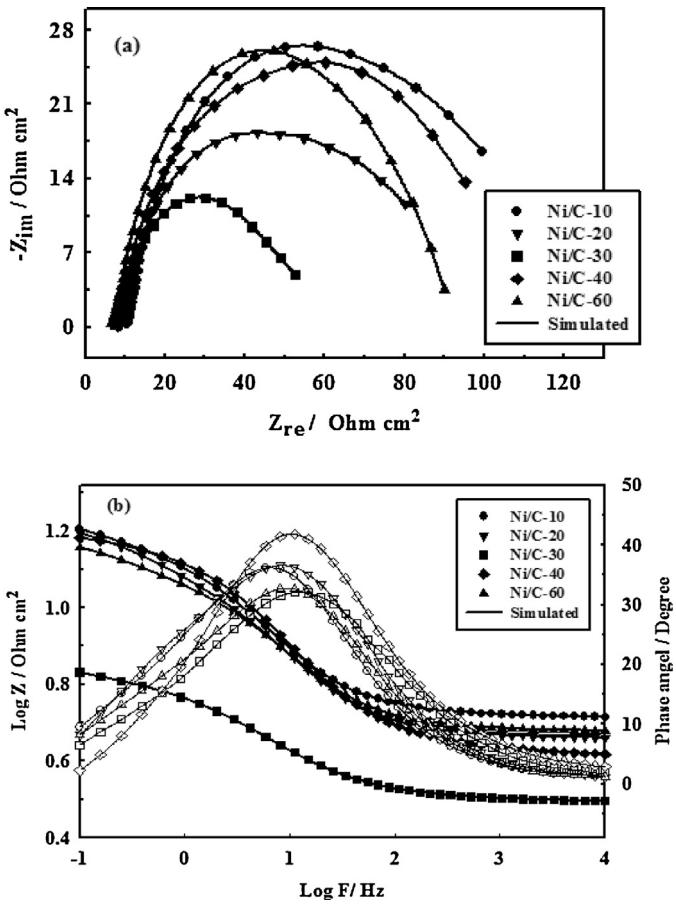

Fig. 12. (a) Nyquist and (b) Bode plots of Ni/C electrocatalysts, containing different nickel weight percentages, in (0.4 M methanol + 0.5 M KOH) solution at 500 mV.

the highest one is for Ni/C-c. The Nyquist plot shows a capacitive loop in high frequency region and follows a small straight line in low frequency region [Ni/C-c electrocatalyst]. The high frequency capacitive loop is related to the charge transfer resistance [37]. On the other hand, the low frequency straight line implies that the methanol oxidation process is diffusion-controlled at Ni/C electrocatalysts heated for longer microwave times [38]. The corresponding Bode plots are shown in Fig. 14b. Two phase maxima at intermediate and low frequency values are observed. The absence of the impedance plateau and the presence of a second phase maximum at low frequency value confirm the predominance of a diffusion process. The impedance data are analyzed using the equivalent circuit shown in Fig. 15 and the circuit elements are displayed in Table 3. The decreased CPE value of Ni/C-b electrocatalyst is related to the onset of the Faradic oxidation reaction supporting its enhanced electrocatalytic activity [39]. When the heating time of Ni/C electrocatalyst is further prolonged, the impedance value increases. This result is in a good agreement with that obtained by cyclic voltammetric technique.

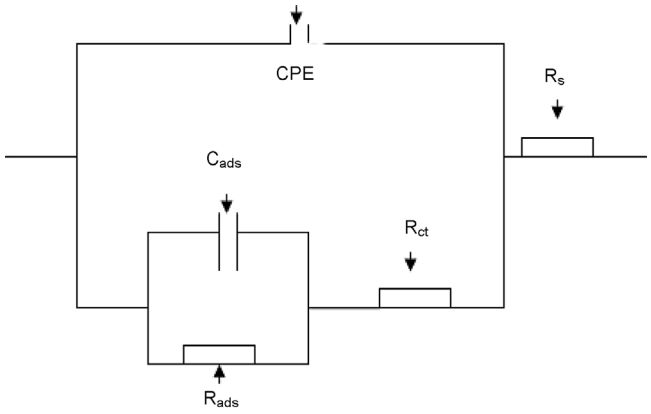

Fig. 13. Electric circuit.

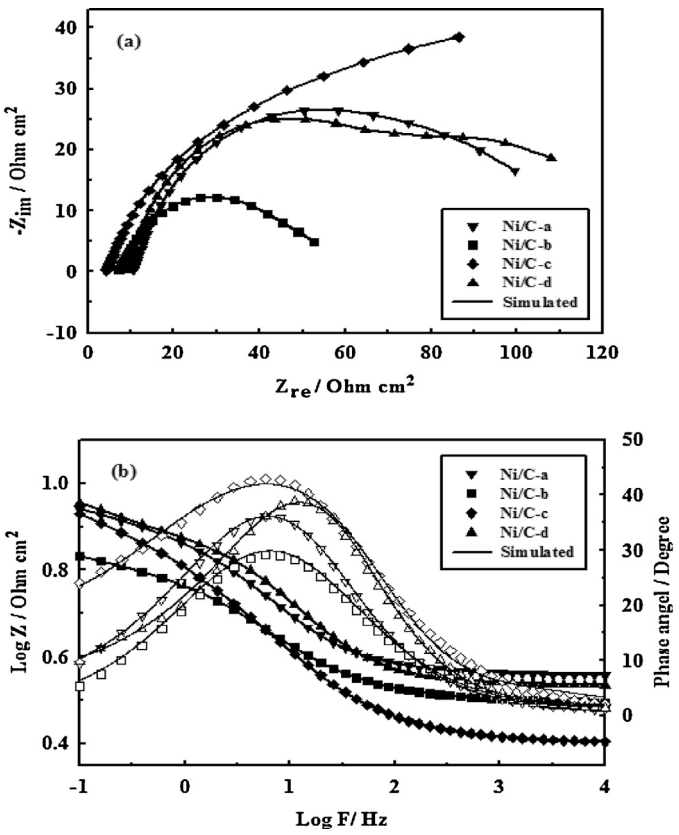

Fig. 14. (a) Nyquist and (b) Bode plots of Ni/C electrocatalysts, heated for different times in microwave oven, in (0.4 M methanol + 0.5 M KOH) solution at 500 mV.

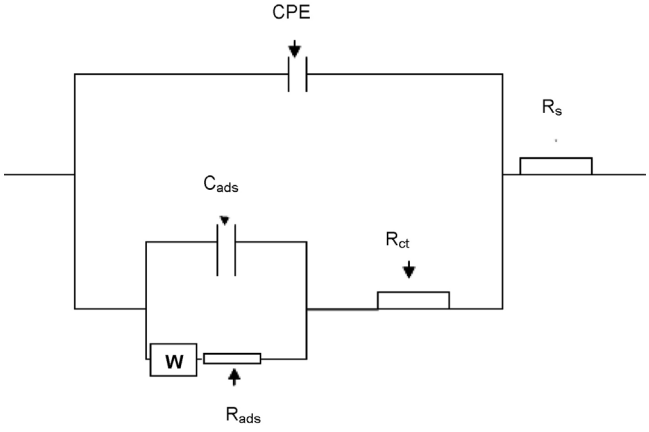

Fig. 15. Electric circuit.

4. Conclusion

1. Nickel nanoparticles were chemically deposited using sodium borohydride as a reducing agent on Vulcan Xc-72R carbon black with the aid of microwave irradiation.
2. TEM images showed that aggregated nickel nanoparticles were formed with increasing the metal weight percentage.
3. The electron transfer coefficient (α) of Ni/C-30 electrocatalyst was estimated as 0.509 with electron transfer rate constant (k_s) of $7.54 \times 10^{-2}\ s^{-1}$.
4. Ni/C electrocatalyst formed using a pulse mode of 20 s on/10 s off is more active than that reduced in 10 s on/10 s off mode by two-folds with a negative shift of its oxidation peak potential by 54 mV.
5. Methanol oxidation reaction at Ni/C electrocatalyst was controlled by OH^- ions concentration with an order value of 1.15.
6. The maximum steady state oxidation current density was attained at Ni/C electrocatalyst containing 40 wt.% Ni, afterwards it declined.
7. The lowest impedance value was recorded for Ni/C electrocatalyst containing 30 wt.% Ni, while the highest one was for Ni/C-10.
8. Increasing the heating time of the pulse mode during nickel ions reduction enhances the electrocatalytic performance of Ni/C electrocatalyst. Nyquist semicircles of Ni/C-b showed the lowest diameter, whereas the highest one was for Ni/C-c.
9. The methanol oxidation process on Ni/C electrocatalysts, heated for longer microwave times, is diffusion-controlled.

References

[1] N.V. Long, M. Ohtaki, T.D. Hien, J. Randy, M. Nogami, Electrochim. Acta 56 (2011) 9133.
[2] P. Strasser, S. Koh, T. Anniyev, J. Greeley, K. More, C. Yu, Z. Liu, S. Kaya, D. Nordlund, H. Ogasawara, M.F. Toney, A. Nilsson, Nat. Chem. 2 (2010) 454.
[3] A. Chen, P. Holt-Hindle, Chem. Rev. 110 (2010) 3767.
[4] Z.-B. Wang, G.-P. Yin, P.-F. Shi, Carbon 44 (2006) 133.
[5] B. Habibi, M.H. Pournaghi-Azar, H. Abdolmohammad-Zadeh, H. Razmi, Int. J. Hydrogen Energy 34 (2009) 2880.
[6] H.J. Salavagione, C. Sanchís, E. Morallón, J. Phys. Chem. C 111 (2007) 12454.
[7] F.S. Hoor, C.N. Tharamani, M.F. Ahmed, S.M. Mayanna, J. Power Sources 167 (2007) 18.
[8] J. Prabhuram, T.S. Zhao, Z.X. Liang, R. Chen, Electrochim. Acta 52 (2007) 2649.
[9] R. Parsons, T. VanderNoot, J. Electroanal. Chem. 257 (1988) 9.
[10] K.-W. Park, J.-H. Choi, K.-S. Ahn, Y.-E. Sung, J. Phys. Chem. B 108 (2004) 5989.
[11] E. Antolini, E.R. Gonzalez, J. Power Sources 195 (2010) 3431.
[12] M. Wang, W. Liu, C. Huang, Int. J. Hydrogen Energy 34 (2009) 2758.
[13] B. Habibi, R. Gahramanzadeh, Int. J. Hydrogen Energy 36 (2011) 1913.
[14] I. Danaee, M. Jafarian, A. Mirzapoor, F. Gobal, M.G. Mahjani, Electrochim. Acta 55 (2010) 2093.
[15] I. Danaee, M. Jafarian, F. Forouzandeh, F. Gobal, M.G. Mahjani, Int. J. Hydrogen Energy 33 (2008) 4367.
[16] A.A. El-Shafei, J. Electroanal. Chem. 471 (1999) 89.
[17] S. Basri, S.K. Kamarudin, W.R.W. Daud, Z. Yaakub, Int. J. Hydrogen Energy 35 (2010) 7957.
[18] Z. Mojović, P. Banković, N. Jović-Jovičić, A. Milutinović-Nikolić, A. Abu Rabi-Stanković, D. Jovanović, Int. J. Hydrogen Energy 36 (2011) 13343.
[19] J. Yang, K. Hidajat, S. Kawi, Mater. Lett. 62 (2008) 1441.
[20] X. Zhang, F. Zhang, R.-F. Guan, K.-Y. Chan, Mater. Res. Bull. 42 (2007) 327.
[21] B. Yang, Q. Lu, Y. Wang, L. Zhuang, J. Lu, P. Liu, J. Wang, R. Wang, Chem. Mater. 15 (2003) 3552.
[22] T.J. Schmidt, M. Noeske, H.A. Gasteiger, R.J. Behm, P. Britz, H. Bönnemann, J. Electrochem. Soc. 145 (1998) 925.
[23] Y. Lin, X. Cui, C.H. Yen, C.M. Wai, Langmuir 21 (2005) 11474.
[24] M. Mastragostino, A. Missiroli, F. Soavi, J. Electrochem. Soc. 151 (2004) A1919.
[25] R.S. Amin, R.M. Abdel Hameed, K.M. El-Khatib, M. Elsayed Youssef, A.A. Elzatahry, Electrochim. Acta 59 (2012) 499.
[26] R.S. Amin, R.M. Abdel Hameed, K.M. El-Khatib, H. El-Abd, E.R. Souaya, Int. J. Hydrogen Energy 37 (2012) 18870.
[27] M. Sakthivel, A. Schlange, U. Kunz, T. Turek, J. Power Sources 195 (2010) 7083.
[28] S. Song, J. Liu, J. Shi, H. Liu, V. Maragou, Y. Wang, P. Tsiakaras, Appl. Catal. B: Environ. 103 (2011) 287.
[29] I. Danaee, M. Jafarian, F. Forouzandeh, F. Gobal, M.G. Mahjani, Int. J. Hydrogen Energy 34 (2009) 859.
[30] I. Danaee, M. Jafarian, F. Forouzandeh, F. Gobal, M.G. Mahjani, Electrochim. Acta 53 (2008) 6602.
[31] E. Laviron, J. Electroanal. Chem. Interfacial. Electrochem. 101 (1979) 19.
[32] A.J. Bard, L.R. Faulkner, Electrochemical Methods. Fundamentals and Applications, second ed., John Wiley & Sons, Inc., New York, NY, 2001.
[33] R.M. Abdel Hameed, Biosens. Bioelectron. 47 (2013) 248.
[34] Y. Wang, D. Zhang, W. Peng, L. Liu, M. Li, Electrochim. Acta 56 (2011) 5754.
[35] M.A. Abdel Rahim, R.M. Abdel Hameed, M.W. Khalil, J. Power Sources 134 (2004) 160.
[36] A. Maritan, F. Toigo, Electrochim. Acta 35 (1990) 141.
[37] S. Majdi, A. Jabbari, H. Heli, H. Yadegari, A.A. Moosavi-Movahedi, S. Haghgoo, J. Solid State Electrochem. 13 (2009) 407.
[38] E. Barsoukov, J.R. Macdonald, Impedance Spectroscopy: Theory, Experiment, and Applications, second ed., Wiley, New Jersey, 2005.
[39] D. Zielinska, B. Pierozynski, J. Electroanal. Chem. 625 (2009) 149.